International Journal of Chemistry and Pharmaceutical Sciences

Journal Home Page: www.pharmaresearchlibrary.com/ijcps

Research Article Open Access

Synthesis, spectral, biological applications on cobalt(III) dithiocarbamate complexes and their solvothermal decomposition to nano cobalt(II) sulphide

A.S. Sonia*, R. Baskaran

Department of Chemistry, Annamalai University, Annamalai Nagar, T.N, India-608 002.

A B S T R A C T

Octahedral diamagnetic $[Co(eedtc)_3]$ (**1**), $[Co(medtc)_3]$ (**2**), $[Co(bhpdtc)_3]$ (**3**) and $[Co(cedtc)_3]$(**4**) (where eedtc = N-ethyl-N-(2-hydroxyethyl) dithiocarbamate anion, medtc = N-methyl-N-(2-hydroxyethyl) dithiocarbamate anion, bhpdtc =N-benzhydryl piperazine dithiocarbamate anion and cedtc = bis(2-cyanoethylamine) dithiocarbamate anion) have been prepared. The synthesized complexes **1**-**4** are characterized by elemental analysis, thermal analysis and spectroscopic methods (IR, UV-Vis and ^{1}H & ^{13}C NMR). The IR spectra suggest the coordination of dithiocarbamate occurred through the two sulphur atoms in a symmetrical bidendate fashion. Electronic spectra of the complexes show signature bands corresponding to d-d transition. One electron quasi reversible reductions which are due to Co (III)/Co (II) redox process are observed in cyclic voltammetry. Final residue obtained in thermal analysis is CoS, indicates the reduction of Co(III) → Co(II). A non conventional solvothermal formation of CoS nano particles is reported with cobalt dithiocarbamate as single source precursor. Morphology and composition of the nano product have been characterized by pXRD, SEM and EDX analysis. The antibacterial activities of synthesized complexes were studied against two gram negative species, *Escherichia coli*, *Pseudomonas aeruginosa* and three gram positive species, *Streptococcus pyogenes*, *Staphylococcus aureus* and *Bacillus subtilis* and for in vitro antifungal activity against *Aspergillus flavus*, *Aspergillus niger*, *Fusarium oxysporum*, *Penicillium chryogenum and Trigoderma veride*.

Keywords: dithiocarbamate, cobalt (III), thioureide, decomposition study, biological applications, nano sulfide

A R T I C L E I N F O

CONTENTS

Article History: Received 21 October 2016, **Accepted** 25 November 2016, **Available Online** 27 November 2016

***Corresponding Author**
A.S. Sonia
Department of Chemistry,
Annamalai University,
Annamalai Nagar, India-608 002.
Manuscript ID: IJCPS3194

PAPER-QR CODE

Citation: A.S. Sonia. Synthesis, spectral, biological applications on cobalt (III) dithiocarbamate complexes and their solvothermal decomposition to nano cobalt (II) sulphide. *Int. J. Chem, Pharm, Sci.*, 2016, 4(12): 616-624.

1. Introduction

Dithiocarbamates are a class of versatile binding agents which coordinate with transition, main group, lanthanide and actinide elements predominantly in a bidentate mode [1-5]. They can be used as antioxidants for increasing the longevity and photo-stability of a variety of polymers, oils and other materials [6]. The symbiotically induced softness and the electronic effects of the substituents on the dithiocarbamate ligands are important factors in deciding the reactivity [7,8]. Due to the metal-chelating properties of dithiocarbamates, they exhibit valuable effect in medicines for the treatment of bacterial, fungal infections [9]. Dithiocarbamates have been tested in clinical trials for various indications including HIV [10,11]. DTCs were recently reported as potent cell apoptosis inhibitors [12]. Commercially, DTCs are well known for their application such as NO trapping agents, lubricants, vulcanizers and solar control devices [13-15]. Furthermore, DTC ligands are used as reagents for the extraction of metals from different mineral acids, and their complexes are utilized as precursor materials in the synthesis of sulfide nanoparticles in modern electronics [16–18].

DTCs are capable of stabilizing metals in a wide range of oxidation states. This is due to the different resonance forms, and the delocalization of the nitrogen lone pair onto the sulfurs. Consequently, cobalt can be present in + 1, + 2, +3 and +4 states [19]. Cobalt (II) DTCs undergoes spontaneous oxidation into the corresponding cobalt (III) compounds. Apart from the propensity of DTC ligands to stabilize relatively higher oxidation states, the larger ligand field stabilization energy in cobalt (III) complexes (a d6 system) also play an important role [20]. In this view, the present work reports the synthesis, characterization of cobalt (III) dithiocarbamate complexes, as well as their thermal stability studies and biological activity in inhibiting the growth of bacterial and fungal strains. In addition to this, complex (2) was used as a single source precursor in the preparation of metal sulfide nano particles which was characterized by powder XRD, SEM and EDX.

2. Materials and Methods

All reagents and solvents were commercially available analytical grade materials and were used as supplied. IR spectra were recorded on an ABB Bomen MB 104 spectrometer (4000-500 cm-1) as KBr pellets. Hitachi U-2001 UV-vis spectrophotometer was used for recording the electronic spectra of the complexes. The ^{1}H NMR and ^{13}C spectra were recorded on Bruker AMX-400 spectrometer operating at 400 MHz and 100.6MHz respectively. TMS is used as internal standard. DMSO and $CDCl_3$ are used as a solvent. Cyclic voltammetric studies were carried out using a CH1604C electro chemical analyzer. Glassy carbon was used as working electrode and the counter electrode was a platinum wire. The reference electrode was Ag/AgCl. Tetrabutyl ammonium per chlorate (0.01 M) was used as the supporting electrolyte. The experiments were carried out under oxygen free atmosphere by bubbling purified nitrogen gas through the solution at room temperature. Thermal analysis was carried out in air on a STA 409 PC thermal science instruments. Powder X-ray diffraction intensities were collected in the 2θ range 2–80° using Bruker-D8 X-ray diffractometer equipped with Cu-Kα radiation at fixed current and potential. Samples were finely powdered and mounted on glass slides. The scan speed and step size were 0.05min and 0.00657 respectively. Scanning electron micrographs of the samples were recorded with JOEL JSM-5610Lv microscopes.EDX was obtained on a JEOL EX-6360A spectrometer at 120eV.

Antibacterial assay (disc diffusion method)

The disc diffusion assay was used to determine antibacterial activity of the complexes using gram positive bacteria viz., *Streptococcus pyogenes, Bacillus subtilis, Staphylococcus aureus* and gram negative bacteria viz., *Escherichia coli* and *Pseudomonas aeruginosa.* Base plates were prepared by pouring 10 mL of autoclaved Muller-Hinton agar into sterile petridishes (9 cm) and allowed them to settle. Sterile blank discs (6 mm) were impregnated with 15 mL of known concentration of stock solution of tested complexes as to obtain discs containing 100 and 400 mg of each complex. Impregnated discs were air dried and cautiously placed on the surface of Muller-Hinton agar plates freshly inoculated with microorganisms. After 10 min at room temperature the plated culture incubated for 24 h at 37°C. Experiments were conducted in quadruplicate (four discs with identical concentration of the same compound) and commercial antibiotic Ciprofloxacin (100 mg) impregnated discs used as positive controls. Susceptibility diameter zone was reported as the average value of replicate measurements.

Antifungal screening (disc diffusion method)

A disc application technique was employed in vitro to evaluate the antifungal activity of synthesized complexes. Antifungal activity of the complexes was tested against Asper*gillus flavus, Aspergillus niger, Fusarium oxysporum, Penicillim chryogenum, Trigoderma veride*. Mature conidia of fungal isolates were harvested from potato dextrose agar (PDA) plates and suspended in ringer solution and spore suspensions standardized with a haemocytometer (104 conidia mL1). Conidial suspension (1mL) representing each fungal isolate was then spread on a 9 cm petridishes containing PDA (20 mL) with the excess of conidial suspension decanted and allow to dry. The compounds were dissolved in dimethyl sulfoxide (DMSO). Sterile 6 mm diameter test discs were impregnated with 15 mL of the solution of each test compound to certain 100 and 400 mg/disc in triplicates. Amphotericin-B was used as a reference drug, for fungal inhibition. While DMSO was used as a negative control. Plates were incubated at room temperature (22-25°C) for 3 days. The radius of the inhibition zone of fungal growth was measured after 3 days. Diameter zone was reported.

Experimental

Synthesis of tris (N-ethyl-N-(2-hydroxyethyl) dithiocarbamato) cobalt (III); [Co(eedtc)$_3$] (1)

2-(ethylamino) ethanol (0.29 ml, 3 mmol) and carbon disulfide (~0.18 ml, 3 mmol) in ethanol (50 ml) was mixed under ice-cold condition (5°C) to form a yellow solution of corresponding dithiocarbamic acid. To the yellow

dithiocarbamic acid solution, an aqueous solution of $CoSO_4$.$7H_2O$ (0.281g, 1mmol) was added with constant stirring. The precipitated dark green complex was filtered, washed with water and was then dried over anhydrous calcium chloride (Yield: 80%. dec.: 295°C). Anal.Calcd for $C_{15}H_{30}N_3S_6O_3Co$: C, 33.37; H, 5.81; N, 8.76. Found: C, 33.43; H, 5.91; N, 8.60 %.

Synthesis of tris(N-methyl-N-(2-hydroxyethyl) dithiocarbamato)cobalt(III);[Co(medtc)$_3$](2)

Prepared similarly using HN (Me) (CH_2CH_2OH) (0.24 ml, 3 mmol), CS_2 (~0.18 mL, 3 mmol) in excess) and $CoSO_4$.$7H_2O$ (0.281g, 1mmol) in water. (Yield: 80%, dec.: 276°C). Anal. Calcd for $C_{12}H_{24}N_3S_6O_3Co$: C, 28.15; H, 5.11; N, 8.01. Found: C, 28.43; H, 5.91; N, 8.60%.

Synthesis of tris(N-benzhydryl piperazine dithiocarbamato) cobalt(III); [Co(bhpdtc)$_3$] (3)

Similarly prepared employing $C_{17}H_{20}N_2$ (0.76 g, 3 mmol), CS_2 (~0.18 mL, 3 mmol in excess) and $CoSO_4$.$7H_2O$. (0.281g, 1mmol) (Yield: 80%, dec.: 301°C). Anal. Calcd for $C_{54}H_{57}N_6S_6Co$: C, 62.17; H, 57.01; N, 8.23. Found: C, 62.43; H, 57.91; N, 8.60%.

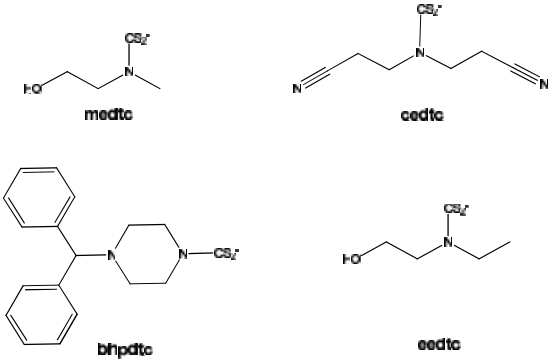

Synthesis of tris(bis(2-cyanoethyl)dithiocarbamato) cobalt (III); [Co(cedtc)$_3$] (4)

Prepared accordingly by reacting HN ($CH_2CH_2CN)_2$ (0.36 mL, 3 mmol), CS_2(~0.18 mL,3 mmol) and $CoSO_4$.$7H_2O$. (0.281g,1 mmol). (Yield: 71% ; Mp. : 241°C) IR (υ/cm 1): 1485 (υ C–N) and 990 (υ C–S). Analysis for $C_{21}H_{24}N_9S_6Co$ Calcd (%): C, 39.21; H, 4.43; N, 19.02. Found (%): C, 39.43; H, 4.91; N, 19.60.

Preparation of CoS nano particles by non-conventional solvothermal decomposition

A mixture of tris (substituteddithiocarbamato) cobalt (III) (1 g) as a clear solution in chloroform (100mL) was heated with diethylenetriamine (2 mL) at 80˚C for 45 min. Solid black nano cobalt sulfide was separated from chloroform, washed with ether, chloroform and the nanoparticles were collected and dried in air. Qualitatively, the ease of formation of nano sulfide from the four cobalt (III)-dithiocarbamates is measured as the time of first appearance of the sulfide on decomposition, which followed the order: **(3)** (340s) > **(4)** (425s) > **(1)** (463s) > **(2)** (489s).

3. Results and Discussion

IR spectral studies: IR spectral data of all the complexes are presented in Table 1. The important characteristic absorptions in the dithiocarbamates are due to υC-N and υC-S stretching modes. Due to the mesomeric shift of electron density from nitrogen towards the metal center increases the contribution of the thioureide form to the structure of the dithiocarbamates, which has been assigned by υC-N band. For complexes (**1**), (**2**), (**3**) and (**4**) the υC-N bands are observed at 1491, 1503, 1489, 1485 cm^{-1}(see Figure 1). Of the four complexes, complex (**2**), shows thioureide band at a higher wave number compared to other complexes (**1**), (**3**) and (**4**) because of the fact that the double bond character in carbon-nitrogen bond is higher for the complex (**2**) compared to others. The υC-S stretching vibration for complexes (**1**), (**2**), (**3**) and (**4**) are observed at 990, 991, 993, 990 cm^{-1} respectively without any splitting supporting the bidentate coordination of the dithiocarbamate moiety [21]. In addition to υC-N and υC-S bands, the spectra showed strong band at 3415 and 3424 cm^{-1} for complex (**1**) and (**2**) due to υO-H band respectively. For complex (**4**), the cyano group is observed at 2922 cm^{-1}.

Electronic Spectroscopy

Electronic spectral data of all the cobalt dithiocarbamate complexes are presented in Table 1. The cobalt (III) complexes are diamagnetic and hence must be in octahedral environment with CoS_6 chromophore. In all the cobalt(III) complexes, bands below 350 nm are due to the intraligand π-π* transitions, mainly associated with the N-C=S and S-C=S groups. The intense band in the 350 - 425 nm region is due to either metal-ligand or ligand-metal charge transfer [22]. Electronic spectral bands in the range of 425 to 650 nm are due to d-d transitions [23]. Electronic spectra of compounds (**1**), (**2**), (**3**) and (**4**) show bands at 645, 641, 642 and 628 (Table 1) respectively, due to d-d transitions. The bands correspond to d-d transition from lower energy d_{xz} level to higher energy dx^2-y^2 level and indicate octahedral geometry around the metal ion. The weak band at 640 nm appears due to the d-d transition (i.e., between d orbitals of CoIII), which is known as a ligand-field (LF) transition. This value is in agreement with the value already found by Venkatesan et al. [24].

NMR spectral studies

The ^1H and ^{13}C NMR chemical shifts of the synthesized complexes are summarized in Table 2. The regions are given for proton and carbon signals and no individual splitting assignments are made.

^1H NMR

In complex (**1**) and (**2**), α-CH_2– and β-CH_2– protons of –CH_2–CH_2–OH appear as broad signals due to the asymmetry in the coordination environment, indicating a substantial barrier to C–N bond rotation.The α –methylene protons of –**CH_2**–CH_2–OH are adjacent to nitrogen of thioureide π system and similarly β -methylene protons of –CH_2–**CH_2**–OH are adjacent to oxygen. Hence, the α and β protons experience strong deshielding and appear as broad singlets in the region 3.41–3.71 ppm for the complexes (**1**) and (**2**). The observed deshielding of the α-CH_2 and β- CH_2 protons in the compounds were attributed to the shift of electron density on the sulphur (or the metal) through the thioureide π system. The OH protons of hydroxyl ethyl group appear as a singlet around 4.96 and 4.99 ppm for (**1**) and (**2**) repectively as expected. In complex (**3**), aromatic

protons resonate in the region of 7.19–7.39 ppm. The γ-methane proton in (**3**) is strongly deshielded due to electron withdrawal effects of two aryl groups and the electronegative nitrogen present at the adjacent position. In the complex (**4**) α –methylene and β-methylene protons of cyano ethyl group the signals were observed at 2.91 and 3.89 ppm respectively (Supplementary material).

^{13}C NMR

For all the complexes (**1)-(4)**, the signals in the downfield region (203.3–206.8 ppm) with low intensity are of thioureide ($N^{13}CS_2$). The slight upfield shift for all the four complexes from normal chemical shift values (206–210 ppm) [25] is due to mesomeric shift of electron density from dtc toward the metal center. The observation is in line with the observation from higher (C–N) in their IR spectra From ^{13}C NMR spectra of the complexes, the chemical shifts of the carbon of thioureide ($N^{13}CS_2$) are correlated to the π bonding in the NCS_2 fragment. Generally, higher υ(C–N) values correlate with lower ($N^{13}CS_2$) chemical shifts for d-block elements. In the hydroxyl ethyl group, α-CH_2 carbon appears to be deshielded to a great extent and the signals were observed at 58.17 and 58.11 ppm for compounds (**1**) and (**2**) respectively and β-CH_2 carbon signals were observed at 30.68 and 11.99 ppm for complexes (**1**) and (**2**) respectively. For (**3**), the methine carbon signal is observed around 75.71 ppm and its deshielding is due to the electronegative nitrogen and the phenyl groups at the α positions. Actually, the methine carbons are strongly deshielded in complex (**3**) and almost overlapping with the solvent signal. Aromatic carbon signals in complex (**3**) are observed in the region of 127.3–141.9 ppm. In the cyano ethyl group, α-CH2 carbon and β-CH2 carbon signals appears to be deshielded to a great extent and the signals were observed at 43.94 and 15.14 ppm for the complex (**4**) respectively. The special characteristic cyano carbon signal of complex (**4**) was observed at 118.10 ppm.

Cyclic voltammetric Studies

CV studies indicate that all the neutral cobalt(III) complexes show large reversible reduction potentials (-1371 mV, -1380 mV,-1317 mV and -1329 mV for (**1**), (**2**), (**3**) and (**4**) respectively) in keeping with their reluctance to add electron density to already electron rich metal centres of the four complexes. The reduced form of the complexes show their readiness to lose electron density as indicated by the higher second reversible oxidation potential values (-1042mV, -1093mV, -1021mV and -993mV) for (**1**), (**2**), (**3**) and (**4**) respectively. Therefore all the neutral cobalt complexes display one quasi-reversible one electron reduction process (ΔE, mV) 329, 287, 296 and 336 (Table 1) for complexes (**1**), (**2**), (**3**) and (**4**) respectively which is assigned to be Co(III) ↔ Co(II) couple [26, 27]. The high negative potential (<-1.0 V) of cobalt (III) – cobalt(II) reduction process can account for the preferential stabilization of cobalt is in +3 oxidation stable in all the cobalt complexes under atmospheric condition.

Thermal decomposition studies

Thermal decomposition of metal dithiocarbamates has been a subject matter of detailed investigation. According to the curves, the complexes decompose in a two-step mechanism. Thermal studies of DTCs suggest that decomposition of these complexes proceeds through the formation of metal thiocyanate intermediates [28], except in a cyclic DTCs or closed rings [29, 30]. Similarly in the present study, the breakdown of DTC moiety occurs followed by the formation of thiocyanate intermediates and metal sulphide as the final product. $[Co(eedtc)_3]$ (**1**) starts to decompose above 200˚C(Table 3) and a single decomposition sets in and proceeds up to 400˚C corresponding to the stabilization of $Co(SCN)_3$ (exptl. : 86.12 % , calcd. : 88.75%). Further in increase temperature leads to the formation of CoS as the final residue (exptl.: 14.8%, calcd.: 17.2%). The experimentally observed values and theoretically calculated values for the mass losses and the end product obtained match within the experimental errors. Thermogram of $[Co(medtc)_3]$ (**2**) indicates the initial loss of CH_3CN solvent molecule at 276˚C (exptl.: 6.18%,calcd.: 5.8%). Immediately after the loss of acetonitrile molecules, subsequently, dithiocarbamate part of 2- methylamino ethanol is burnt upto 368˚C (exptl.: 79.4 %, calcd.: 76.8%). The formation of CoS as a final product around 900˚C (Table 3) is supported by the close agreement of experimental (15.7%) and the calculated (17.8%) mass loss. $[Co(bhpdtc)_3]$ (**3**) starts to decompose around 206˚C, indicating the loss of benzene(exptl.: 10.0% calcd.: 11.6%). Immediately after the loss of benzene, a single decomposition step is observed upto 308˚C corresponding to the stabilization of $Co(SCN)_3$ (exptl.: 8.19%, calcd.: 7.93%).The final residue obtained at 800˚C corresponds to CoS (exptl.: 9.52% , calcd.: 8.83%). $[Co(cedtc)_3]$ (**4**) decompose around 276˚C indicates the loss of dithiocarbamate ligand (exptl.: 64.1 %, calcd.: 66%) followed by the decomposition of $Co(SCN)_3$. CoS is obtained as a final residue (exptl.: 5.1%, calcd.: 6.2%). The experimentally observed values and theoretically calculated values for the mass losses and the end products obtained are in agreement with the proposed formula (Figure 4). All the TG analysis showed that the cobalt (III) complexes conformed to the proposed molecular formulae of the complexes. The final residue obtained in all the process is CoS, which indicates the reduction of Co^{3+} to Co^{2+} during thermal decay [31, 32]. The differential scanning calorimetry (DSC) curves show a small peak around 96˚C due to loss of volatiles. An exothermic peak around 302˚C is associated with the decomposition of the complex, and according to the thermogravimetric analysis (TGA) and differential thermogravimetric (DTG) curves, it corresponds to the peak of maximum rate of the decomposition. Another exothermic peak at 406˚C is associated with the second step of decomposition. The DSC curve showed that there was an intermediate step before the second decomposition, which is not well resolved in the DTG perhaps due to the simultaneous occurrence of the process [33].

Antibacterial studies

The results of the antibacterial activities of the complexes are presented in Table 4 and Figure 6. Five pathogens; *Streptococcus pyogenes, Bacillus subtilis, Staphylococcus aureus, Escherichia coli* and *Pseudomonas aeruginosa* were used in the screening. Significant antibacterial activities were observed when compared to standard drug

ciprofloxacin. Complexes (**1**), (**3**) and (**4**) exhibits less activity (Table 4) against all the tested bacteria. But complex (**2**) is more toxic when compared to other complexes. The resistivity of the ligand by these bacteria could be due to its non permeation through lipid layers of the cell wall bacteria and the detoxification of the compound through the secretion of beta lactamase. Due to the delocalization of the electrons on the ligands, it increases the lipophilic character of the complex, and favours its permeation through lipid layers of the bacterial membrane [34, 35].

Antifungal studies

The antifungal activity of the complexes using amphotericin-B was studied in vitro and results are summarized in Table 5 and Figure 7. Significant antifungal activity was observed for the complexes as compared with that of standard drug ciprofloxacin. Complex (**1**) was found to exhibit maximum activity against *Trigoderma veride* when compared with other complexes. Complexes (**1**) & (**3**) also showed good activity (Table 5) against *Fusarium oxysporum.* All the complexes does not show activity against *Aspergillus niger* except (**4**). Complex (**4**) exhibited more activity against *Penicillium chryogenum.* Complex (**2**) explored good inhibitory activity against *Aspergillus flavus.* The antifungal activity of dithiocarbamates may be attributed to their ability to chelate with metal ions. When these metal complexes penetrates lipid barriers in the fungal cell and may become ultimate toxicant or alternatively it may be converted into free dithiocarbamate anions, which complexing with trace metals and thus depriving the cell of the needed metal ion and therefore causes death of fungal cell.

Characterization of cobalt sulfide

Powder XRD analysis

All the diffraction peaks in the XRD can be indexed for CoS (Figure 5). The strong peaks corresponding to (221), (111) and (200) reflections which are in good agreement with the JCPDS-pattern (JCPDS file No: 89-3056) (Rhombohedral, space group R3m, a = 9.619, c = 3.149) [36]. A very strong peak was appeared at 25 (2θ) due to the presence of mixture of sulphides [CoS_2]. Average diameter of the CoS particles are estimated to be 33 nm by Debye – Scherrer calculation from the PXRD pattern [37].

SEM-EDX analysis

The SEM image shows the agglomeration of particles. Scanning electron micrograph of CoS particles and show a typical EDX pattern of CoS particles (Figure 5). The surface morphology is in the range of 18-31 nm in the SEM. The elemental composition of CoS particles was determined by EDX spectroscopy performing spot measurements on particles. The major peaks are due to the presence of Co along with sulphur. Preparation of nanosheets, nanofilms and nanowires of binary metal sulphides from single source precursors have been reported by making use of chemical vapour deposition, aerosol assisted chemical vapour deposition and thermal decomposition techniques [38-40]. In this report, preparation of nano CoS has been accomplished through a simple solvothermal degradation of the precursor and the particle size distribution is relatively large.

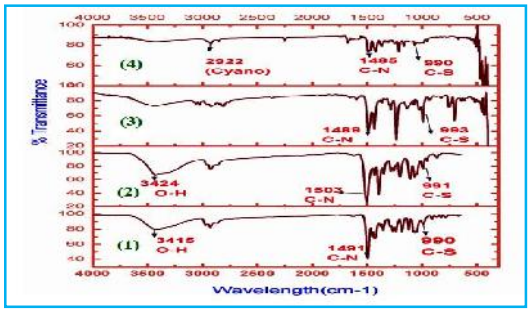

Figure 1: IR spectra of complexes 1-4

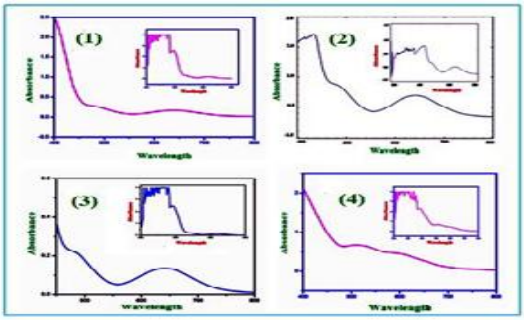

Figure 2: UV-visible spectra of complexes 1-4

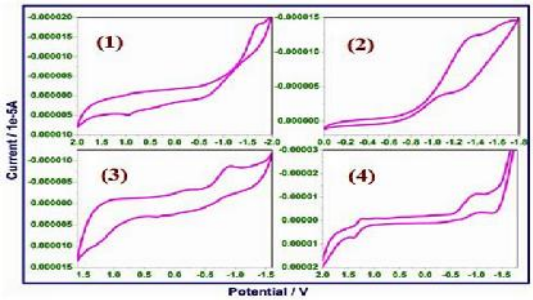

Figure 3: Cyclic voltammetry of complexes 1-4

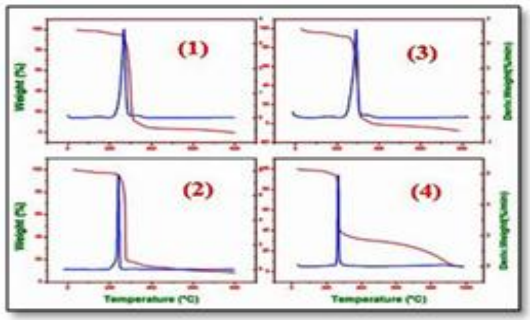

Figure 4: Thermal analysis of complexes 1-4

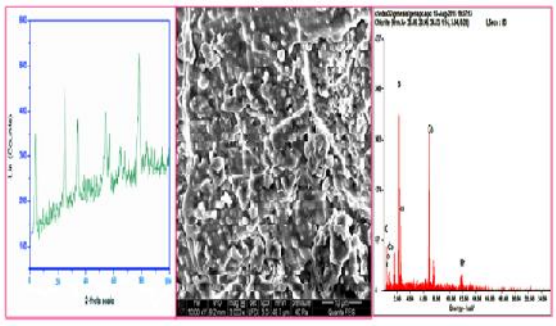

Figure 5: Powder XRD, HRSEM and EDAX of nano Co

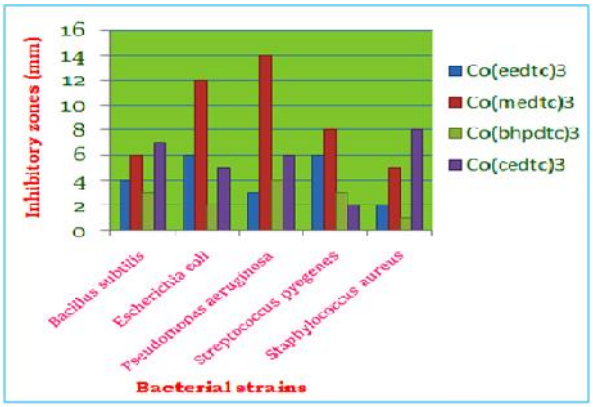

Figure 6: Antibacterial activity of complexes 1-4

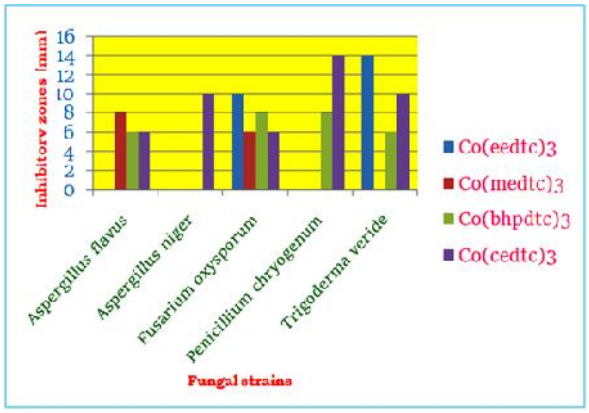

Figure 7: Antifungal activity of complexes 1-4

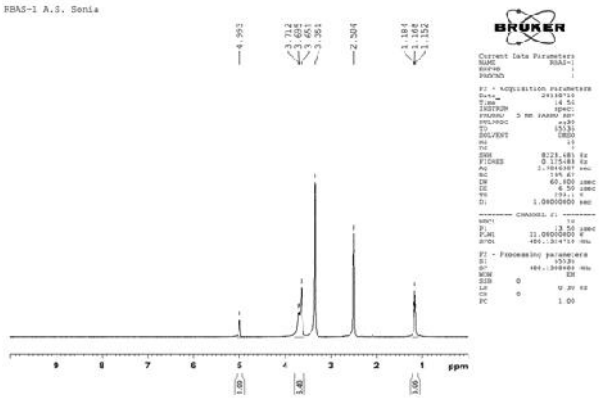

Figure S1: ^{1}H NMR of Co (eedtc)$_3$

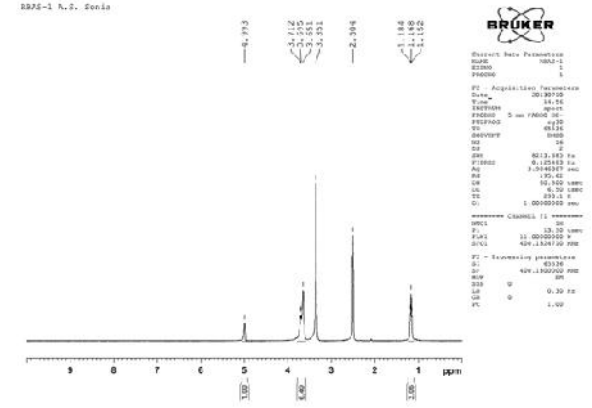

Figure S2: ^{13}C NMR of Co(eedtc)$_3$

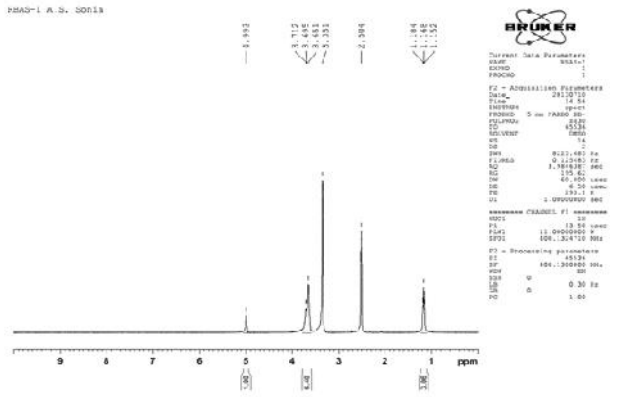

Figure S3: ^{1}H NMR of Co(medtc)$_3$

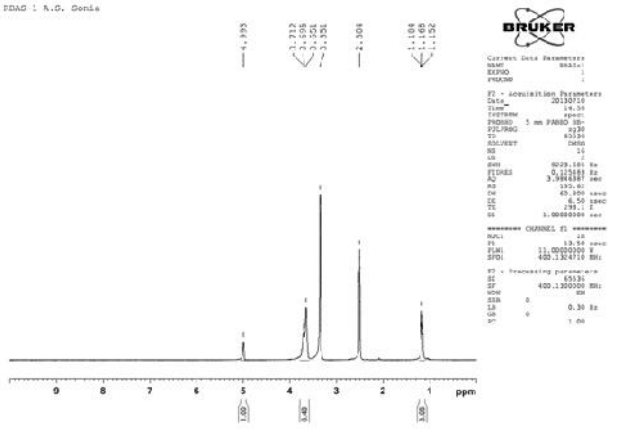

Figure S4: ^{13}C NMR of Co(medtc)$_3$

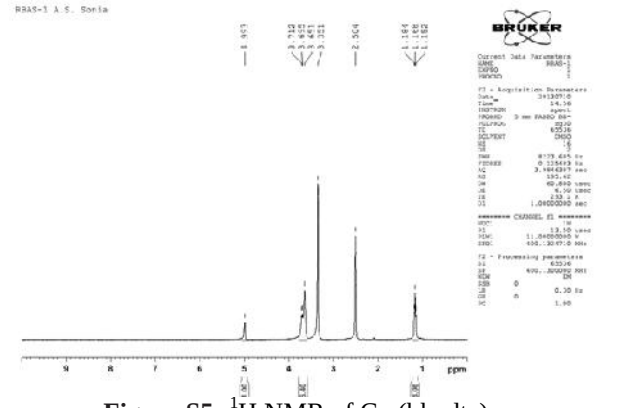

Figure S5: ^{1}H NMR of Co (bhpdtc)$_3$

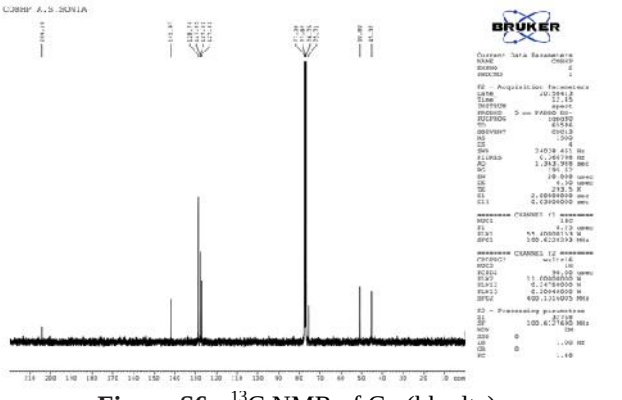

Figure S6: ^{13}C NMR of Co (bhpdtc)$_3$

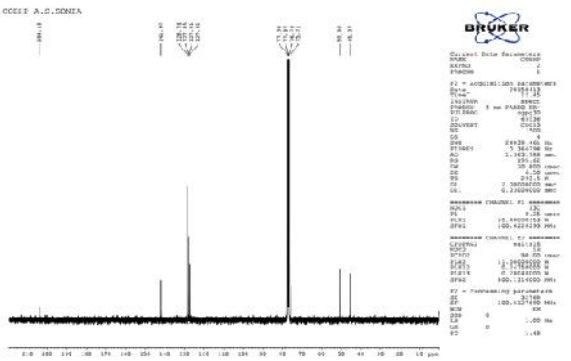

Figure S7: ^{1}H NMR of Co (cedtc)$_3$

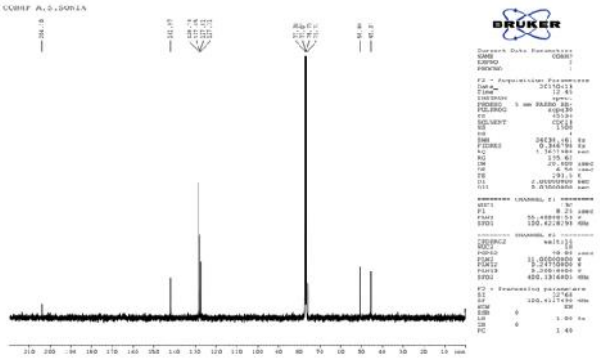

Figure S8: ^{13}C NMR of Co (medtc)$_3$

Table 1: UV, IR and CV spectral data

Complex	UV-Vis(nm) λ_{max}	IR (cm^{-1})			CV (mV)	
		υC-N	υC-S	υO-H/cyano	Reduction	Oxidation
(**1**)	645	1491	990	3415	-1371	-1042
(**2**)	641	1503	991	3424	-1380	-1093
(**3**)	642	1489	993	-	-1329	-1021
(**4**)	628	1485	990	2922	-1380	-993

Table 2: NMR chemical shifts of the complexes (in ppm).

Compound	NMR	~-CH_2–	β-CH_2–	–CH_2 – CH_3/ CH_3/Aromatic/CN	-OH	N $^{13}CS_2$ (Thioureide)
(**1**)	^{1}H	3.65-3.71		1.15-1.18	4.99	
	^{13}C	30.68	58.17	44.26 11.99		203.36
(**2**)	^{1}H	3.41-3.67		2.07-3.19	4.96	
	^{13}C	11.99	58.11	30.68		203.53
(**3**)	^{1}H	Piperazine		7.19-7.39	–	
	^{13}C	α ,β	α', β'	141.91 77.38		204.1
		3.85	2.453			
		50.80	45.37			
(**4**)	^{1}H	2.44-3.94			–	
	^{13}C	15.14	43.94	118.10		206.89

Table 3: Thermogravimetric data

Complex	MW	Mass loss %		Decomposition range	Fragment lost/end product*
		exptl.	cacld.		
[Co(eedtc)$_3$] (**1**)	299.0	86.1	88.7	200˚C-400˚C	Decomposition of eedtc, $Co(SCN)_3^*$, C_2H_5OH
		17.3	19.2	600˚C -900˚C	CoS^*
[Co(medtc)$_3$] (**2**)	276.4	6.1	5.8	276˚C	-CH_3CN
		73.6	73.0	276˚C -368˚C	Decomposition of medtc, $Co(SCN)_3^*$, C_2H_5OH
		15.5	19.7	>900˚C	CoS^*
[Co(bhpdtc)$_3$] (**3**)	301.8	8.3	7.6	206˚C	C_6H_6
		87.1	83.8	206˚C -308˚C	Decomposition of bhpdtc, $Co(SCN)_3^*$,$Co(NCS)(CN)^*$
		10.7	9.1	>800˚C	CoS^*
[Co(cedtc)$_3$] (**4**)	265.87	64.1	66	263-268 ˚C	Decomposition of cedtc, $Co(SCN)_3$
		5.1	6.2	>900˚C	CoS^*

Table 4: Antibacterial activity table for the complexes (**1-4**).

S.No	Bacterial Strains	Standard drug*	Zone of inhibition (mm)			
			(1)	(2)	(3)	(4)
1.	*Bacillus subtilis*	12	04	06	03	07
2.	*Escherichia coli*	16	06	12	02	05

3.	*Pseudomonas aeruginosa*	18	03	14	04	06
4.	*Streptococcus pyogenes*	14	06	08	03	02
5.	*Staphylococcus aureus*	08	02	05	01	08

***Ciprofloxacin**

Table 5: Antifungal activity table for the complexes (1-4).

S.No	Fungal Strains	Standard drug*	Zone of inhibition (mm)			
			(1)	(2)	(3)	(4)
1.	*Aspergillus flavus*	22	00	08	06	06
2.	*Aspergillus niger*	22	00	00	00	10
3.	*Fusarium oxysporum*	28	10	06	08	06
4.	*Penicillium chryogenum*	24	00	00	08	14
5.	*Trigoderma veride*	26	14	00	06	10

***Amphotericin-B**

4. Conclusion

New complexes **1**-**4**, have been synthesized, characterized by elemental analysis and spectroscopic studies. The spectral data obtained are consistent with the proposed composition, with the DTCs coordinating in a symmetrical bidentate fashion. A simple solvothermal method for the synthesis of CoS nanoparticles is reported. Information on the size, morphology and composition of the product are obtained by powder XRD, SEM and EDX analysis. The average size of prepared NiS nano particles is 31 nm. The high to moderate activities of the synthesized complexes against both bacterial and fungal strains proved their usefulness as potential antibacterial and antifungal agents.

5. References

[1] RP Feazell, CE Carson, KK Klausmeyer. Variability in the structures of [4-(aminomethyl) pyridine] silver(I) complexes through effects of ligand ratio anion, hydrogen bonding and p stacking. *Inorg. Chem.*, 2006, 45: 935-944.

[2] PJ Heard, KD Karlin. Main group dithiocarbamate complexes. *Prog. Inorg.Chem.*, 2005, 53: 1-612.

[3] G Hogarth. Metal dithiocarbamate complexes: chemistry and biological activity. *Mini Rev. Med. Chem.*, 2012, 12: 1202-1215.

[4] S Sivasekar, K Ramalingam, C Rizzoli, N Alexander. Continuous shape measure and bond valence sum characterization of bismuth (III) complexes of substituted dithiocarbamates and solvothermal decomposition. *Inorg. Chim.Acta.*, 2014, 419: 82-88.

[5] GS Sivagurunathan, K Ramalingam, C Rizzoli. Continuous shape measure of electronic effect free steric distortions in tris(dithiocarbamato) indium (III): synthesis, spectral, electrochemical, single crystal Xeray structural investigation and BVS calculations on tris (dithiocarbamato) indium(III) complexes. *Polyhedron*., 2014, 72: 96-102.

[6] R Becker, A Knorr. An evaluation of antioxidants for vegetable oils at elevated temperatures. *Lubr. Sci.*, 1996, 8**:** 95-117.

[7] AH Norbury. Coordination Chemistry of the Cyanate, Thiocyanate, and Selenocyanate Ions. *Adv. Inorg. Chem.*, 1975, 17: 231-386.

[8] K Ramalingam, G Aravamudan, V Venkatachalam, Production of Thiosulfate Anion from the Reaction of Bis (dialkyldithiocarbamato) nickel (II) Complexes with Ethylenediamine *Bull. Chem. Soc. Jpn.*, 1993, 66 (5): 1554-1555.

[9] DC Onwudiwe, PA Ajibade. ZnS, CdS and HgS Nanoparticles via Alkyl-Phenyl Dithiocarbamate Complexes as Single Source Precursors *Int. J. Mol. Sci.*, 2011, 12: 5538-5551.

[10] S Fujii, T Yoshimura. A new trend in iron–dithiocarbamate complexes: as an endogenous NO trapping agent. *Coord. Chem. Rev.*, 2000, 198: 89-99.

[11] RJ Levine. Multicenter, randomized, placebo-controlled study of dithiocarb (Imuthiol) in human immunodeficiency virus-infected asymptomatic and minimally symptomatic patients. AIDS *Res. Hum. Retrov.*, 1993, 9(1): 83-89.

[12] EM Hersh, G Brewton, D Abrams, J Bartlett, J Galpin, P Gill, R Gorter, M Gottlieb, JJ Jonikas, S Landesman. Dithiocarb sodium (diethyl dithiocarbamate) therapy in patients with symptomatic HIV infection and AIDS: a randomized, double-blind, placebo-controlled, multicenter study. *JAMA.*, 1991, 265(12): 1538-1544.

[13] KS Siddiqia, S Khan, SAA Nami, MM El-ajaily. Polynuclear transition metal complexes with thiocarbohydrazide and dithiocarbamates. *Spectrochim Acta Part A.*, 2007, 67(3): 995-1002.

[14] NA Law, W Dietzsch, NV Duffy. A multinuclear (1H, 13C, 15N) NMR study of cis-halonitrosyl bis (dithiocarbamato)iron(II) complexes: effect of replacement of S by Se. *Polyhedron*., 2003, 22: 3423–3432.

[15] JM Lo, JD Lee. Dithiocarbamate extraction and Au (III) back extraction for determination of mercury in water and biological samples by anodic stripping voltammetry. *Anal Chem.*, 1994, *66*(8): 1242-1248.

[16] G Barone, T Chaplin, TG Hibbert, AT Kana, MF Mahon, KC Molly, ID Worsley, IP Parkin, SP Louise. Synthesis and thermal decomposition

studies of homo- and heteroleptic tin(IV) thiolates and dithiocarbamates: molecular precursors for tin sulfides. *J Chem Soc Dalton Trans.,* 2002, 1085–1092.

[17] N Revaprasadu, SN Mlondo. Use of metal complexes to synthesize semiconductor nanoparticles. *Pure Appl Chem.*, 2006, 78 (9): 1691–1702.

[18] MD Regulacio, N Tomson, SL Stoll. Dithiocarbamate precursors for rare-earth sulfides. *Chem Mat.*, 2005, 17 (12): 3114–3121.

[19] G Hogarth. Transition metal dithiocarbamates. *Prog Inorg Chem.*, 2005, 53: 71– 561.

[20] BS Manhas, BC Verma, SB Kalia. Spectral and magnetic studies on normal cobalt (II) planar and cobalt (III) octahedral, spin-crossover cobalt (III) octahedral and planar-tetrahedral cobalt (II) carbodithioates. *Polyhedron.*, 1995, 14(23): 3549-3556.

[21] F Bonati and R Ugo. Organotin (IV) N,N' disubstituted dithiocarbamates. *J. Organomet. Chem.*, 1967, 110: 527.

[22] K Ramalingam, G Aravamudan and M Seshasayee. Cyclic voltammetric and infrared spectral studies on the interaction of Ni (II) dithiocarbamates with triphenylphosphine and the crystal and molecular structure of diethyl dithiocarbamatobis (triphenylphosphine) nickel (II) perchlo-rate [Ni(dedtc) $(PPh_3)_2$] ClO_4. *Inorg. Chim.Acta.,* 1987, 128 (2): 231-237.

[23] MV Rajasekaran, GVR Chandramouli and PT Manoharan. Polarized electronic spectral studies on some diethyldithiocarbamate complexes of Ni (II) and Pd (II). *Chem. Phys. Lett.*, 1989, 162 (1): 110-116.

[24] KA Venkatesan, TG Srinivasan, PR Vasudeva Rao. Cobalt-extraction studies on dithiocarbamate grafted on silica gel surface. *Colloids Surf., A*, 2001, 180 (3): 277-284.

[25] HLM Van Gaal, JW Diesveld, FW Pijpers, JGM Van Der Linden. Carbon-13 NMR spectra of dithiocarbamates, chemical shifts, carbon-nitrogen stretching vibration frequencies and pi-bonding in the NCS_2 fragment. *Inorg. Chem.*, 1979, 18: 3251-3260.

[26] RB Lanjewar and AN Garg. Synthesis, electronic, infrared and mossbauer spectroscopic studies of mixed-ligand complexes of monocarbamato and bis (n, n'-diethyldithio-carbamato) iron (iii) with o, n and s containing chelating ligands and their thermal-decomposition. *Indian J. Chem.*, 1992, 31(11)**:** 849-854.

[27] KS Siddiqui, SA Nami, LY Chebude. Template synthesis of symmetrical transition metal dithiocarbamates. *J. Braz. Chem. Soc.*, 2006, 17 (1): 107-112.

[28] D Ondrusova, E Jona, P Simon. Thermal properties of N-ethyl-N-phenyl-dithiocarbamates and their influence on the kinetics of cure. *J Therm Anal Calorim.*, 2002, 67 (1): 147–152.

[29] ET Cavalheiro, M Ionasshiro, G Marino, ST Breviglieri, GO Chierice, The effect of the aminic substituent on the thermal decomposition of cyclic dithiocarbamates. *J Braz Chem Soc.*, 1999, 10(1): 65–75.

[30] VD Benedini, PA Antunes, ETG Cavalheiro, GO Chierice. Thermoanalytical and solution stability studies of hexamethylene dithiocarbamates. *J Braz Chem Soc.*, 2006, 17: 680–688.

[31] YH Wen, HM Zhang, P Qian, HT Zhou, P Zhao, BL Yi, YS Yang. A study of the Fe (III)/Fe (II)–triethanolamine complex redox couple for redox flow battery application. *Electrochim. Acta.*, 2006, 51 (18): 3769-3775.

[32] TJ Hubin, JM Mc Cormick, NW Alcock, DH Busch. Topologically constrained manganese (III) and iron (III) complexes of two cross-bridged tetraazamacrocycles. *Inorg. Chem.,* 2001, 40 (3): 435-444.

[33] DC Onwudiwe, JN Mugo, M Hrubaru, E Hosten. Bis diallyl dithiocarbamate Pt (II) complex: synthesis, characterization, thermal decomposition studies, and experimental and theoretical studies on its crystal structure. *J. of Sulfur Chemistry.*, 2015, 36: 36–47.

[34] AA Osowole, GA Kolawole, R Kempe, OE Fagade. Spectroscopic, Magnetic and Biological Studies on Some Metal (II) Complexes of 3-(4, 6-Dimethyl-2Pyrimidinylamino)-1-Phenyl-2-Butenone and the Mixed Complexes with 2, 2′-Bipyridine and 1, 10-Phenanthroline. *Sythn. React Inorg Met-Org Chem.*, 2009, 39(3): 165–174.

[35] AA Osowole, AO Daramola. Synthesis, physicochemical and Biological activities of some metal (II) complexes of (methylsulfanyl)-2, 4-benzenediol Schiff base. *Elixir Appl Chem.*, 2011, 39: 4876–4879.

[36] Joint Committee on Powder Diffraction Standards [JCPDS], File No 75-0613.

[37] H Klug and LE Alexander, X-Ray Diffraction Procedures for polycrystalline and amorphous material, New York, John Wiley, 1974.

[38] H Nabipour. Synthesis of a new dithiocarbamate cobalt complex and its nanoparticles with the study of their biological properties. *Int. J.Nano. Dim*., 2011, 3: 225-232.

[39] RB Rakhi, NA Alhebshi, DH Anjum and HN Alshareef. Nanostructured cobalt sulfide-on-fiber with tunable morphology as electrodes for asymmetric hybrid Supercapacitors. *J. Mater. Chem. A.*, 2014, 2: 16190–16198.

[40] G Wang, S Zhuo. Hierarchical micro/nano-structured cobalt sulfide spindles as low-cost counter electrodes for dye-sensitized solar cells. *Phys. Chem. Chem. Phys.*, 2013, 15: 13801-13804.